Kinetic Basis for the Substrate Specificity during Hydrolysis of Phospholipids by Secreted Phospholipase A_2[†]

Joseph Rogers,[‡] Bao-Zhu Yu,[‡] Spyros V. Serves,[§] Gerasimos M. Tsivgoulis,[§] Demetrios N. Sotiropoulos,[§] Panayiotis V. Ioannou,*[,§] and Mahendra Kumar Jain*[,‡]

Department of Chemistry and Biochemistry, University of Delaware, Newark, Delaware 19716, and Department of Chemistry, University of Patras, Patras, Greece

Received March 4, 1996; Revised Manuscript Received May 31, 1996[⊗]

ABSTRACT: Kinetics of hydrolysis of aqueous dispersions of arsono-, sulfo-, phosphono- and phospholipids by phospholipase A_2 from pig pancreas are characterized in terms of interfacial rate and equilibrium parameters. The enzyme with or without calcium binds with high affinity to the aqueous dispersions of the four classes of anionic lipids and shows the same general kinetic behavior. The rate of hydrolysis of anionic substrates does not show an anomalous change at the critical micelle concentration because the enzyme is present in aggregates even when bulk of the substrate is dispersed as a solitary monomer. Apparent affinities of the enzyme for the interface of different anionic lipids are virtually the same. Also, affinities of these substrates for the active site of the enzyme at the interface are comparable. However, a significant change in the catalytic turnover rate is seen as the *sn*-3 phosphodiester group is modified; the apparent maximum rate at saturating bulk substrate concentration, V_M^{app} values, increase in the order: homo- and arsonolipids < sulfo- < phosphono- < phospholipids. Not only the basis for the *sn*-2 enantiomeric selectivity but also the decrease in the rate of hydrolysis with the increasing chain length is due to a decrease in the value of V_M^{app}. Results show that even when the bulk concentration of anionic phospholipid is below cmc, hydrolysis occurs in aggregates of enzyme and substrate where the chemical step of the turnover cycle remains rate-limiting, which provides a basis for the assumption that V_M^{app} is directly related to k_{cat}. The fact that k_{cat} depends on the nature of the head group (phosphate, phosphonate, sulfate, arsonate) implies that the head group plays a critical role in the rate-limiting chemical step of the catalytic cycle, possibly during the decomposition of the tetrahedral intermediate. The significance of these results for the microscopic steady-state condition for hydrolysis at the micellar interface, mechanism of esterolysis by phospholipase A_2, and inhibitor design are discussed.

The role of calcium as a catalytic cofactor for phospholipase A_2 (PLA_2)[1] (Verheij et al., 1980; Yu et al., 1993) is supported by a variety of observations. In the crystal structure of PLA_2 calcium is coordinated to seven oxygen ligands: two from the carboxyl group of Asp-49, three from the peptide carbonyls of residues Tyr-28, Gly-30, and Gly-32, and two from water molecules (Dijkstra et al., 1983). In cocrystals of PLA_2 with substrate mimics (Scott et al., 1990; Thunnissen et al., 1990) the water ligands are replaced by two oxygens of the mimic: the apical water (w_{12}) by *pro-S* oxygen atom of the *sn*-3 phosphate and the equatorial water (w_5) by the oxygen of the *sn*-2 substituent to form a pentagonal bipyramidal complex. The role of the *sn*-3 phosphate in the binding of the substrate to the catalytic site is also implicated by structure−activity correlation for substrate analogs (Kuipers et al., 1990). Nevertheless, quantitative interfacial equilibrium binding studies with substrate mimics without the *sn*-3 phosphate or equivalent polar substituent (Jain et al., 1991b, 1993b), such as MJ33 (Figure 1), suggest that although calcium is an obligatory cofactor for their binding to the active site of PLA_2, the *sn*-3 phosphate is neither necessary nor does it contribute significantly toward the thermodynamic stability of the complexes. This is surprising because the binding energy for the active site-directed ligand to the enzyme in the interface is believed to come largely, if not exclusively, from the head group interactions of the ligand with the active site (Kuipers, 1990; Jain et al., 1993b).

To characterize the head group interactions in the formation of the ternary Michaelis complex and in the transition state, and to understand the role of calcium as a cofactor in the catalytic cycle of PLA_2, we investigated kinetic and equilibrium properties of arsono-, phosphono-, sulfo-, and phospholipids as substrates. In this paper we describe

[†] This work was supported by Research Grant GM29703 (to M.K.J.) from the National Institutes of Health.

* To whom correspondence should be addressed.

[‡] University of Delaware.

[§] University of Patras.

[⊗] Abstract published in *Advance ACS Abstracts,* July 15, 1996.

[1] Abbreviations: BAPTA, 1,2-bis(*o*-aminophenoxy)ethane-*N*,*N*,*N*′,*N*′-tetraacetic acid; cmc, critical micelle concentration; PxB, polymyxin B sulfate; PLA_2, secreted phospholipase A_2 from bovine or pig pancreas unless indicated otherwise; Quin-2, 2-[[2-[bis[(ethoxycarbonyl)methyl]-amino]-5-methylphenoxy]methyl]-6-methoxy-8-[bis-[(ethoxycarbonyl)-methyl]amino]quinoline; DC_nX, structures and abbreviations for phospho-, phosphono-, and arsonolipids as well as for the inhibitors (MJ33 and RM2) are given in Figure 1; dithiophospholipids are the corresponding 1,2-dithioesters; the ether analogs are 1,2-dialkylglycerophospholipids. Definition of parameters at the interface: K_{Ca}*, dissociation constant for Ca^{2+} determined by the protection method; K_{Ca}*(S), effective dissociation constant for Ca^{2+} under catalytic conditions at a mole fraction of 1 of the substrate; K_I*, dissociation constant of inhibitor; K_M*, Michaelis constant; K_P* dissociation constant of product; K_S* dissociation constant of substrate; k_{cat}, turnover number at saturating substrate concentration; v_0, turnover number at $X_S = 1$; X_I, mole fraction of inhibitor. For complete analytical formalism and definitions, see Berg et al. (1991) and Jain et al. (1995).

S0006-2960(96)00526-0 CCC: $12.00

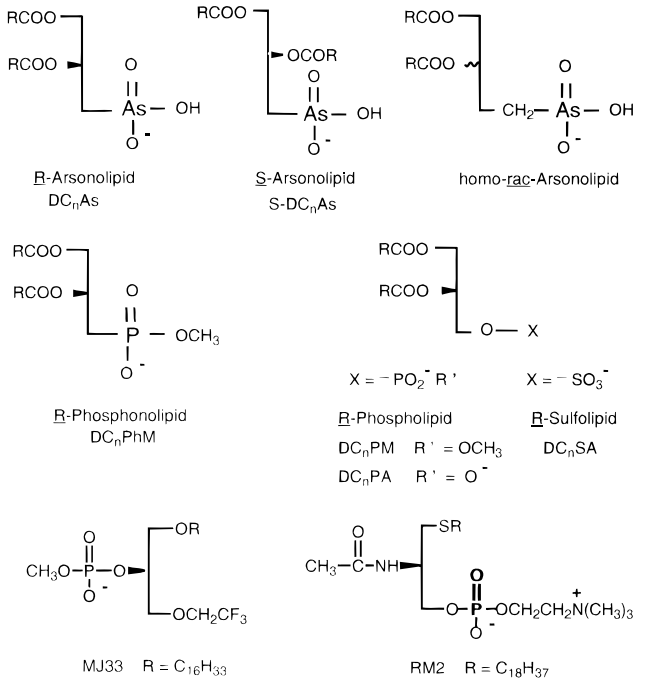

FIGURE 1: Structures of substrates (phospho-, sulfo-, phosphono-, and arsonolipids) and active site-directed inhibitors (MJ33 and RM2) used in this study.

protocols for the characterization of interfacial kinetic and equilibrium parameters on micelles, and the methods are applied to study the effect of changing the structure of the *sn*-3 substituent on the phospholipid substrate. Results show that although equilibrium binding behavior of arsonolipids and phospholipids is comparable, arsonolipids have considerably lower k_{cat}.

MATERIALS AND METHODS

Sources of enzymes, reagents and experimental protocols were the same as those described before (Yu et al., 1993; Jain et al., 1991a). PxB was purchased from Sigma Co. and DC_nPA (monosodium salt) from Avanti Polar Lipids. DC_n-SA (Eibl, 1980), DC_nPM-ether, DC_8PM (Jain & Rogers, 1989), and MJ33 (Jain et al., 1991b) were synthesized as described. Sources for the following are gratefully acknowledged: RM2 from Dr. Ronald Magolda (DuPont Co., Wilmington, DE), and dithio-DC_8 PM from Professor H. Stewart Hendrickson (St. Olaf College, Northfield, MN).

Synthesis of Lipids. 2,3-Dioctanoyloxypropyl chloride was prepared by acylation of 3-chloro-1,2-propanediol with octanoyl chloride in the presence of pyridine in dry chloroform for 10 days. The reaction mixture was processed by washing the mixture with water, dilute sulfuric acid, water, and saturated sodium bicarbonate, and then the organic layer was concentrated by removal of chloroform. The product was purified by chromatography on silica gel.

The dimethyl ester of (rac)-2,3-dioctanoyloxypropane-1-phosphonic acid was synthesized by Arbuzov reaction of trimethyl phosphite (8.4 mmol) with (rac)-2,3-dioctanoyloxyiodopropane (3.75 mmol) in an oil bath at 135 °C for 20 h. After cooling, the reaction mixture was chromatographed on silica gel with petroleum ether with increasing proportion of diethyl ether; the product eluted with 100% diethyl ether (10% yield). The dimethyl ester was demethylated with lithium bromide to obtain DC_8PhM. The method of Rosenthal et al. (1975) did not work in our hands; 50−90% diacyloxyhalopropanes were recovered following the reaction of tris(trimethylsilyl) phosphite with diacyloxychloro- or diacyloxyiodopropanes at 130 °C for 18 h.

Synthetic protocols developed earlier were adopted for the synthesis of *R*- and *S*-DC_nAs from 2,3-dihydroxypropyl-1-arsonic acid (Tsivgoulis et al., 1991; Lacoste et al., 1992; Serves et al., 1992). Neutral or acid salts (with tetrabutylammonium counterion) of the 2,3-dihydroxypropyl-1-arsonic acid were acylated by acid anhydrides (Tsivgoulis et al., 1991; Serves et al., 1992). Alternately, the phenyl esters of *R*- or *S*-dihydroxypropylthioarsonous acids were acylated by acid chlorides (Serves et al., 1993). The second method affords better yields and is better suited for the synthesis of short chain arsonolipids.

The enantiomeric purity of arsonolipids was judged on the basis of the extent of hydrolysis by PLA_2. For this purpose the hydrolysis of arsonolipids by PLA_2 was carried out in wet diethyl or diisopropyl ether dispersions where the progress of the reaction was monitored by thin layer chromatography. Under these conditions only the *sn*-2 chain of the *R*- but not of the *S*-arsonolipids is cleaved, and the reaction proceeded to completion. Based on these criteria, the stereochemical purity of the arsonolipids used in this study is better than 95% (Serves et al., 1992, 1993).

The phosphono-, arsono-, sulfo- and phospholipids were pure by TLC and NMR criteria. Physical properties of the aqueous dispersions of phosphono- and arsonolipids were similar but not identical to those of the corresponding phosphatidic acid and phosphomethyl ester. As is the case with phospholipids, the long chain arsonolipids form lamellar phases which show the characteristic gel−fluid thermotropic transition (Serves et al., 1992, 1993). Also, as is the case with the phosphatidylmethanol analogs (Jain & Rogers, 1989), the short chain phosphono- and arsonolipids in aqueous dispersions are in monomeric form below their respective cmc's, and above cmc there will be an equilibrium between the monomeric and micellar form of lipid. Although there appears to be no effect of cmc on the profile of v_0 versus concentration of anionic substrates, cmc appears to have an effect on certain interfacial parameters, such as X_1-(50). Cmc determinations are, therefore, necessary to obtain an accurate estimate of these parameters.

Moreover, there are noticeable differences in some of the physical properties of the dispersions of phosphono- and arsonolipids. For example, homophosphonolipids exhibit significantly decreased solubilities and ability to disperse in aqueous phase (Schwartz et al., 1988), and dispersions of arsonolipids are somewhat more turbid. This would be expected if these dispersions showed polymorphism as seen with phosphatidylcholines with acyl chain lengths of eight or nine carbon atoms (Tausk et al., 1974; Lewis et al., 1990; Soltys & Roberts, 1994). In short, the physical behavior of dispersions of arsonolipids is comparable to those of homologous phosphonolipids with one or two more methylene residues.

Determination of Cmc. Cmc was determined on a Roller-Smith surface tension balance (Du Nouy ring design) in 4 mL of 100 mM NaCl, 1 mM $CaCl_2$, 10 mM Tris buffer at pH 8.0. Solutions were stirred after addition of each aliquot of lipid before measuring surface tension.

Binding of PLA_2. Binding of PLA_2 to lipid dispersions was determined by several methods. Binding of pig pancreatic

PLA_2 (1.2 μM) to DC_8PM-ether was monitored as the change in fluorescence at 333 nm (excitation at 280 nm) on a SLM-Aminco AB2 Luminescence Spectrometer with magnetic stirring in a cuvette containing 1.5 mL of 100 mM NaCl, 1 mM $CaCl_2$, and 10 mM Tris, pH 8.0. Typically, the slit widths were kept at 4 nm each, and the sensitivity (PMT voltage) was adjusted to 1% for the Raman peak corresponding to the same excitation wavelength from the buffer blank. The relative change in fluorescence, δF, is defined as $(F - F_0)/F_0$, where F_0 and F are the intensity without and with phospholipid, respectively. The change in the absorbance spectrum and related measurements under conditions specified in the text were carried out on HP8452 UV−vis diode array spectrophotometer.

Kinetic Protocols. Analytical formalism and protocols developed for the kinetic and equilibrium binding studies with vesicles of anionic phospholipids (Berg et al., 1991; Jain et al., 1986a, 1991a, 1995) are adopted to characterize the kinetics of hydrolysis of the micellar dispersions of short chain arsono-, phosphono-, and phospholipids by PLA_2. Arsonolipids (powders) were dispersed by sonication (Sonicor) in aqueous 100 mM NaCl and adjusted to pH 8.0 with sodium bicarbonate. Salts of other lipids were dispersed in water, and concentrations of stock solutions were verified by the extent of hydrolysis by PLA_2 in pH-stat assays. Hydrolysis of aqueous dispersions of lipids was initiated with PLA_2 and monitored by the pH-stat method using a Brinkman (Metrohm) assembly with a stirrer speed about 2000 rpm. Unless stated otherwise, pH-stat experiments were carried out in 4 mL of 100 mM NaCl and 1 mM $CaCl_2$ at 25 °C and pH 8.0 under a stream of nitrogen (Jain et al., 1986a; Berg et al., 1991). In order to prevent precipitation, it was necessary to assay DC_8PA in 0.3 mM $CaCl_2$; nonetheless, this concentration is sufficient for full catalytic activity [see K_{Ca}*(S) value in Table 2]. Typically, 1−35 pmol of enzyme was used to initiate the reaction, depending on the V_M^{app} of the substrate. Hydrolysis commenced in less than 3 s after addition of enzyme to any of the substrate dispersions reported here. To prevent carryover of enzyme, the reaction vessel was washed with detergent, rinsed several times with water, washed with hydrogen peroxide, and finally rinsed several times with water. Background drift rates were typically less than 1 nmol/min and were insignificant (typically <1%) compared to the measured catalytic rates. If inhibitor or other components were present in the reaction mixture, they were added before initiating the reaction with enzyme; however, controls showed that the sequence of addition of most components in the micellar assays did not significantly affect the appearance of the reaction progress curve. The initial rate is expressed as turnover number per second, with uncertainty in reported values less than 10%. Standard deviation for the derived parameters is 15%.

Background calcium levels of various solutions were tested by fluorescence titration with Quin-2 (Tsien & Pozzan, 1989) or by titrating the reaction mixture with BAPTA, which has very high affinity for Ca. Both methods gave comparable results and showed background calcium to be in the 1−100 μM range, depending on the substrate and other additives. Experiments with DC_8PM to determine K_{Ca}*(S), the effective dissociation constant of calcium in the presence of a substrate interface, were performed without or buffered with a chelating agent (EGTA). For experiments without EGTA, the Ca(II) concentration was adjusted by adding the background Ca concentration, estimated at 5 μM, to values on the *x*-axis as in Figure 3. K_{Ca}*(S) values from the two methods were in agreement.

Several methods were tried to completely eliminate the background levels of calcium. None were entirely satisfactory; however, the background level of calcium in the salt solution could be reduced routinely to less than 5 μM by passing the salt solution used for the reaction through Chelex (Sigma). The best method to minimize background calcium in the lipid solution was to pass the methanol solution of the lipid through a column of CM-Sephadex cation exchanger, which had been washed with 0.25 M HCl and then with 4 M NaCl passed through Chelex, and then equilibrated in methanol. Even with these precautions, rates, which could be eliminated by the addition of BAPTA, showed that background calcium concentration in the reaction vessel was about 1 μM.

Kinetic and Equilibrium Parameters. Detailed kinetic studies were carried out with pig and bovine pancreatic PLA_2. Except for small but significant quantitative differences, results were qualitatively the same. The reaction progress was recorded as appropriate for obtaining the zero-order initial rate (v_o) at various bulk concentrations of lipid; for long-chain analogs, 20−40 μg of PxB was added [see Cajal et al. (1996) and Jain et al. (1991c)]. DC_{14}PA presented a special case. Since PxB has no effect on replenishment of DC_{14}PA and concentrations of calcium needed to induce fusion also induce precipitation, large vesicles obtained by freezing and thawing of the sonicated dispersions were used, and v_0 was calculated from curve fit of the first order reaction progress curve [see Berg et al. (1991)]. For long-chain analogs, v_0 does not change with bulk concentration of lipid because the enzyme is catalyzing hydrolysis in the scooting mode, whereby the enzyme does not leave the vesicle to which it is bound. Thus, V_M^{app} values for long-chain lipids in Table 2 are v_0, i.e., the initial rate at the maximum possible mole fraction of the substrate at the interface, $X_S = 1$. K_M^{app} values for the short-chain substrates were obtained from plots of v_0 versus (total) bulk substrate concentration; again, K_M^{app} has no meaning for long-chain analogs. $X_I(50)$ values, the mole fraction of inhibitor required for 50% inhibition of v_0, were measured at saturating substrate concentrations. These values are calculated by assuming that all the inhibitor is distributed in lipid micelles or in the outer monolayer of vesicles present in the reaction mixture (i.e., bulk concentration−cmc for lipid in the case of micelles; or the concentration of lipid in the outer monolayer of vesicles, typically 70% of the bulk concentration for small, sonicated vesicles). Typically, results were obtained by adding successive aliquots of inhibitor solution to the reaction mixture. Controls showed that the order of addition of the enzyme, substrate, calcium, or inhibitor had no anomalous effect on inhibition kinetics.

Equilibrium dissociation constants for the substrate analog (K_S*), products of hydrolysis (K_P*), and inhibitors (K_I*) were determined by the protection method (Jain et al., 1991a; Yu et al., 1993). Values of the interfacial equilibrium parameters are expressed in mole fraction units, and the estimated uncertainty in these values is less than 30%. Analytical relationships and procedures for calculating derived parameters are given in the text. Detailed experimental protocols for the determination of equilibrium dissociation constants for inhibitors bound to E or E* have been described (Jain et

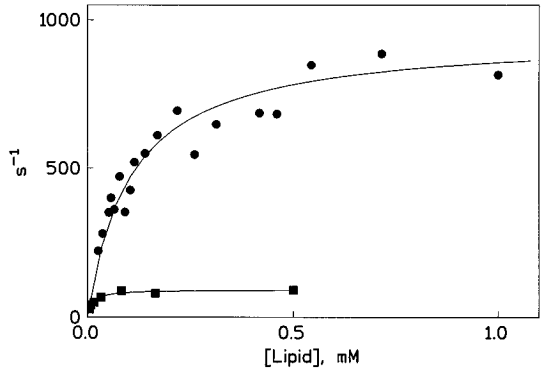

FIGURE 2: Rate versus total bulk lipid concentration for DC_8PM (circles) and 1,2-dithio-DC_8PM (squares) by bovine PLA_2 in 4 mL of 100 mM NaCl and 1 mM $CaCl_2$ at 25 °C and pH 8.0.

al., 1991a,b). As indicated in the text and shown elsewhere (Berg et al., 1991; Jain et al., 1995) from combinations of these parameters, it is possible to obtain values of interfacial K_M* and k_{cat} parameters for the hydrolysis of $DC_{14}PM$ vesicles in the scooting mode.

RESULTS

Kinetic Features of the Hydrolysis of Short-Chain Anionic Lipids. As shown earlier (Jain & Rogers, 1989), the initial region of the reaction progress curve for the hydrolysis of the aqueous dispersions of DC_8PM is pseudo-zero-order. The same is true for other short-chain anionic substrates. Key results for the bovine and porcine PLA_2's are reported here. The reaction begins immediately after the addition of enzyme, and all the substrate present in the reaction mixture is eventually hydrolyzed with a decreasing rate characteristic of integrated Michaelis reaction progress. Intrinsic enzyme activity remains undiminished as is evident when a fresh aliquot of substrate is added to the reaction mixture at the end of the reaction progress curve. In addition, measured rates show a linear dependence on the concentration of enzyme added. These kinetic boundary conditions distinguish this micellar assay from others used for interfacial catalysis (Jain et al., 1995; Gelb et al., 1995).

The initial rate of hydrolysis of the short-chain anionic phospholipids exhibits a hyperbolic dependence upon the bulk substrate concentration (Figure 2). As shown, the most remarkable feature of the hydrolysis of DC_8PM is that the rate of hydrolysis shows no anomalous change in the observed rate at the cmc. Such a behavior is quite unlike that seen for the hydrolysis of zwitterionic short chain phosphatidylcholines (de Haas et al., 1971; Pieterson et al., 1974; Jain & Rogers, 1989). The initial rate of hydrolysis increases with the chain length and the nature of the head group. For example, v_0 at the bulk saturating concentration of DC_4PM is 4.5 s^{-1} compared to ~1000 for DC_8PM. Also, we could not detect any hydrolysis of DC_4PA nor did it inhibit hydrolysis of other phospholipids, although it did promote binding of PLA2 to zwitterionic interfaces. The kinetic basis for such effects is elaborated below.

At saturating concentrations of DC_8PM, the chemical step remains rate-limiting as shown by comparing the rate of hydrolysis with that of its 1,2- dithioester analog (Figure 2 and Table 1): the ratio of the rates of hydrolysis of the oxy- versus thio- analog of DC_8PM at saturating substrate concentrations is 10. This oxy/thio ratio or O/S element effect is comparable to that observed for the hydrolysis of longer chain substrate in the processive scooting mode (Jain et al., 1992). The magnitude of this effect shows that even though the rate of hydrolysis of DC_8PM is about 950 s^{-1} with bovine PLA_2, it is still limited by the chemical step. As shown for mixed micelles of long-chain phospholipids, if the substrate replenishment during the hydrolysis was limited by physical factors such as exchange or diffusion, the rates of hydrolysis of the oxy- and thio- analogs would be virtually the same [for example, see Jain et al. 1993a)].

Table 1: Kinetic and Equilibrium Parameters for the Hydrolysis of DC_8PM by Bovine Pancreatic PLA_2 in 0.1 M NaCl and 1 mM $CaCl_2$ in the Presence of Two Active Site-Directed Inhibitors

	oxy	thio
V_{max}^{app} (s^{-1})	990	92
K_M^{app} (μM)	100	11
K_{Ca}*(S) (μM)	3.7	
K_{Ca}* (μM)	300	
K_M* from K_{Ca}*(S)	0.012	
$X_I(50)^a$ MJ33	0.5	
RM2	0.3	
K_I* MJ33	0.01	
RM2	0.007	
K_M* from MJ33	0.01	
from RM2	0.016	
k_{cat} (s^{-1})	1000	

[a] Values are taken above cmc of DC_8PM (Figure 4C).

Hydrolysis of Arsonolipids by PLA_2. The kinetic behavior for the hydrolysis of arsonolipids was similar to that for anionic phosphono- or phospholipids. The possible origin of the difference in the observed rate was characterized by structure−activity correlation and by monitoring the catalytic parameters (Table 2). The apparent binding affinity of PLA_2 to interfaces of the various lipids (expressed as K_M^{app}) is within a factor of 2, whereas the maximum observed rate at saturating bulk substrate concentrations, V_M^{app}, differ by more than a factor of 400. As shown later, this difference is due primarily to a difference in the interfacial k_{cat} parameter.

In addition to the arsenic versus phosphorus substitution, the structure of DC_8As differs from DC_8PM in two important respects (Figure 1): in DC_8As the oxygen bridge to the backbone is missing and it is dianionic. The relative contribution of such factors can be judged from the following considerations. As shown in Table 2, the rates (V_M^{app}) for the hydrolysis of DC_8PhM and DC_8PA are about 3-fold lower than that of DC_8PM. Therefore, V_M^{app} for the hydrolysis of dioctanoyl glycerophosphonate (which could not be synthesized) is expected to be about 10-fold lower, about 120 s^{-1}. Since the observed rate for DC_8As is 20 s^{-1}, it may be concluded the net effect of substitution of phosphorus by arsenic is about a 6-fold lower rate. The arsonolipids with four oxygen substituents to arsenic, isosteric with phospholipids, cannot be synthesized by existing methods and are expected to be unstable (Long & Ray, 1973). Therefore, homoarsonolipid with a methylene substituent was synthesized (Serves et al., 1995). Its rate of hydrolysis could not be measured titrimetrically; however, as described below, its dispersions in ether−water mixture are susceptible to hydrolysis by PLA_2. Collectively these results suggest that the effect of changing the *sn*-3 substituent on V_M^{app} is incremental and small but significant.

Table 2: Kinetic Parameters with Pig Pancreatic PLA_2 with Various Short-Chain, Anionic Substrates in 100 mM NaCl/1 mM $CaCl_2$

group	DC_8PM $-OPO_3CH_3$	DC_8PA $-OP_3H$	DC_8PhM $-PO_3CH_3$	DC_8As $-AsO_3H$	$DC_{10}As$ $-AsO_3H$	$DC_{12}As$ $-AsO_3H$	$DC_{14}SA$ $-OSO_3H$	$DC_{14}PA$ $-OP_3H$	$DC_{14}PM$
V_M^{app} (s^{-1})	1260	420	380	20	5	3	40	40	300
K_M^{app} (μM)	160	240	100	120					
K_{Ca}*(S) (μM)	6	10	10	6	40		100		100
K_M*[a]	0.02	0.034	0.034	0.02	0.015		0.67		0.67
X_I(50) (MJ33)	0.086	0.0147		0.051	0.027	0.017	0.003	0.003	0.006
K_M*	0.015	0.10		0.027	0.053	0.088	0.67	0.87	0.30
k_{cat} (s^{-1})	1280	450	390	20	6	3	75	80	450
K_S*	0.004				0.023				0.017
K_P*	0.025				0.013				0.03

[a] Based on K_{Ca}* = 0.3 mM.

Enantiomeric selectivity for arsonolipids was the same as for phospholipids: in aqueous as well as wet diethyl ether dispersions, only the *R*- but not the *S*-isomer was hydrolyzed by PLA_2. This is based on the observation that the appearance of the products by thin layer chromatography [in chloroform and acetic acid 10:1 v/v)] on silica plate (Analtach) or by proton release under pH-stat titration conditions was observed only with the *R*-isomer but not with the *S*-isomer. Hydrolysis of $DC_{14}As$ and homo-$DC_{14}As$ could be monitored only in wet diethyl ether dispersions; here rates of reaction were too slow to monitor effectively with pH-stat titrations. Only *R*-isomers of all the lipid classes, including the homoarsonolipids, were hydrolyzed.

Hydrolysis of Arsonolipids by PLA₂'s from Other Sources. Arsonolipids are also hydrolyzed by PLA_2 from other sources. Essentially the same features of hydrolysis of arsonolipids by pancreatic PLA_2 as described above were observed with type II (2 s^{-1} with the human synovial enzyme and 1.1 s^{-1} with the basic *Agkistrodon halys Blomhoffi* venom enzyme) and type III (1.6 s^{-1} with the enzyme from bee venom) PLA_2 with $DC_{10}As$ substrate. In all cases the rate of hydrolysis was dependent on substrate, calcium, and enzyme concentration as well as on the chain length of the substrate. Only the *R*-isomer was hydrolyzed, and as detailed below inhibition was observed in the presence of active site-directed inhibitors.

Kinetic Features of the Hydrolysis of Long-Chain Anionic Lipids. As shown in Table 2, the trends for long-chain anionic lipids are the same as those for short-chain anionic lipids. Changing the head group from a phosphatidylmethanol to the corresponding phosphatidic acid reduces the rate by a factor of 4. Substituting sulfur for phosphorus in this monoester has no further effect on the rate. Yet, it should be noted that $DC_{14}SA$ is monoanionic as opposed to the dianionic $DC_{14}PA$. The rates of hydrolysis for $DC_{14}As$ were immeasurably slow, at least a factor of 100 lower than the rate of $DC_{14}PM$. This is consistent with the assertion that a 4-fold decrease in the rate is due to the change to a dianionic lipid, then another 4-fold change is due to substitution of phosphorus by arsenic, and then a comparable change is due to the removal of the *sn*-3 oxygen in the arsonate.

Kinetic and Equilibrium Parameters. As developed below, the formalism developed for anionic vesicles (Berg et al., 1991; Jain et al., 1995) was modified to consider whether the enzyme involved in the catalytic turnover is actually sampling monodispersed solitary substrate molecules or the Michaelis complex is in an aggregate form even when the bulk substrate is monomeric. In the first case K_M^{app} and V_M^{app} have standard enzymological significance for the catalytic turnover cycle. Since aggregated species of large molecular weight are formed in a mixture of PLA_2 with anionic phospholipids below their critical micelle concentration, it would appear that under virtually all the conditions with which we are concerned the kinetic behavior is in accord with the constraints of catalytic turnover at the interface of a small aggregate.

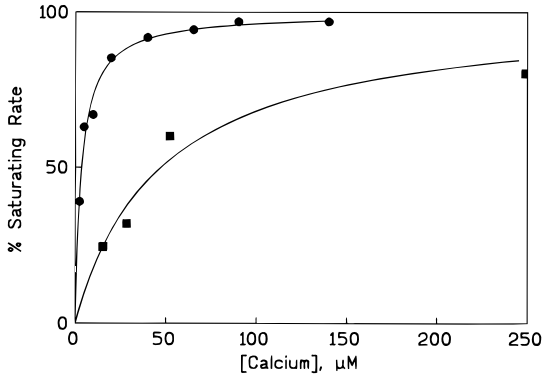

FIGURE 3: Dependence of the rate of hydrolysis of DC_8PM (circles) $DC_{10}As$ (squares) by pig pancreatic PLA_2 on the calcium concentration. The lipid concentration was 1 mM in both cases. Calcium concentrations are corrected for the background Ca(II). Other conditions are as in Figure 2.

Determination of Interfacial K_M.* Calcium is an essential cofactor for the hydrolysis of phospholipids, arsonolipids, and phosphonolipids by PLA_2. As shown in Figure 3, the rates of hydrolysis of DC_8PM or $DC_{10}As$ show a hyperbolic dependence on the calcium concentration although the corresponding V_m^{app} values differ by more than a factor of 250 (Table 2). Values of the apparent kinetic dissociation constant for calcium in the presence of a substrate interface, K_{Ca}*(S), obtained from such plots are summarized in Tables 1 and 2. They show a relatively small variation with the structure of the head group, even though the maximal rates (V_M^{app}) at saturating calcium concentration show a much larger range. K_{Ca}*(S) is related to K_{Ca}*, the dissociation constant for calcium bound to PLA_2 at the interface but without the substrate in the active site. Since K_{Ca}* is obtained independently by the protection method, it is possible to calculate interfacial K_M* from eq 1 (Yu et al., 1993):

$$K_{Ca}^*(S) = \frac{K_{Ca}^*}{1 + \frac{X_S}{K_M^*}} \quad (1)$$

Assuming that the mole fraction of the substrate at the interface, $X_S = 1$, calculated K_M* values are summarized in Tables 1 and 2.

K_M* values were also obtained from the kinetics of inhibition in the presence of active site-directed competitive inhibitors such as MJ33 and RM2 (Jain et al., 1991b). Hydrolysis of DC_8PM is inhibited by these inhibitors. The order of addition of the components of the reaction mixture was not critical, and the same degree of inhibition was seen whether substrate was preequilibrated with inhibitor before the addition of enzyme or when the inhibitor was added to reaction in progress. As expected, the competitive inhibitor changes only the initial rate of hydrolysis but not the extent of hydrolysis. The plot of v_o/v_I ratio versus the inhibitor concentration is linear; here, v_o is the steady-state rate in the absence of inhibitor, and v_I is the rate in the presence of inhibitor. With all the substrate and inhibitor combinations that we have tested, the plot was linear with greater than 90% inhibition at higher concentrations of the inhibitor. The bulk concentration of an inhibitor for 50% decrease in the rate, $I_c(50)$ values, were obtained from such plot.

The dependence of $I_c(50)$ values on the bulk concentration of DC_8PM was particularly revealing. As shown in Figure 4A, $I_c(50)$ value increases with the bulk substrate concentration with an abrupt change at 0.4 mM, which corresponds to the cmc of DC_8PM. Results below cmc are replotted in Figure 4B. For the action of a soluble enzyme on a soluble monomeric substrate

$$I_c(50) = K_I + \frac{K_I[S]}{K_M} \qquad (2)$$

Calculated values of K_I and K_M for several inhibitors were compared. The calculated value of K_M were comparable but somewhat larger than the experimental K_M^{app}. On the other hand, the calculated K_I values are considerably smaller than the corresponding K_L value but comparable to the K_L^{eff} values obtained at the interface of a neutral diluent. Based on these and other (Rogers et al., 1992; Jain et al., 1993b) results, it can be assumed that even though the bulk substrate concentration is below the critical micellar concentration, the environment that the complex of the enzyme and the inhibitor "sees" is similar to that of the complex bound to the interface of a neutral diluent. Such anomalies are also indicated by other kinetic results (Rogers et al., 1992), and spectroscopic evidence is presented in the next subsection.

For the interpretation of results in Figure 4A, consider the following arguments. Below cmc, bulk of the substrate is monodisperse; however, the enzyme in the premicellar aggregate has its own complement of substrate molecules which will determine the effective substrate concentration in the organized (micro-)interface. Inhibitors that we have tested are expected to partition almost completely into any premicellar aggregates that may be formed below the critical micellar concentrations of the substrate. This will result in an effectively higher concentration of the inhibitors on the enzyme containing aggregate. This is because only a small fraction of the total substrate is in the aggregate, and the enzyme containing micelle sequesters a much larger proportion of the inhibitor, i.e., the enzyme in the premicellar aggregate "sees" a much higher mole fraction of the inhibitor than that based on the bulk average concentration of the inhibitor.

The low $I_c(50)$ values observed at the sub-cmc bulk concentrations of DC_8PM are consistent with this interpretation, and so is the fact that $I_c(50)$ does not increase significantly until cmc of DC_8PM is reached (Figure 4A). As expected, below cmc an increase in the bulk substrate concentration does not change the effective substrate or inhibitor mole fraction in the premicellar aggregate. Only above cmc of DC_8PM, where there are sufficient micelles of lipid, is a uniform and random distribution of inhibitor throughout the bulk ensemble of micelles ensured. Thus a constant $X_I(50)$ is seen only above cmc.

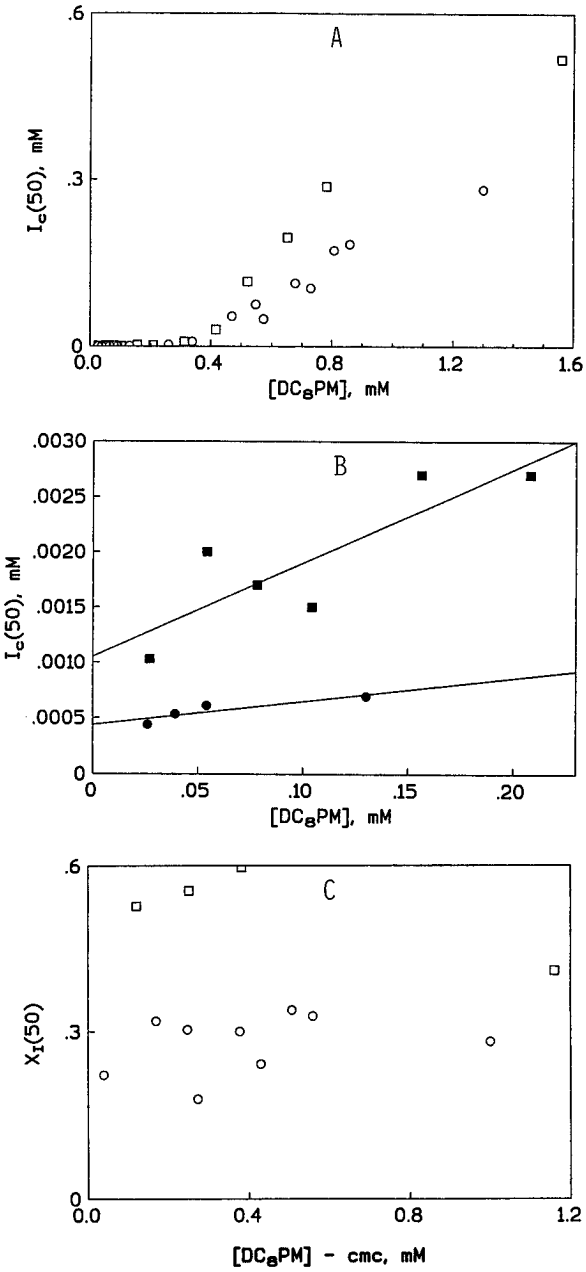

FIGURE 4: (A) Dependence of $I_c(50)$ for MJ33 (squares) and RM2 (circles) on the bulk concentration of DC_8PM. Reaction conditions were as in Figure 2. (B). Expanded scale for the dependence of $I_c(50)$ for MJ33 (squares) and RM2 (circles) on the concentration of DC_8PM below its cmc value. K_I is obtained as the *y*-intercept of this plot if it is assumed that the catalytic turnover is described by the classical soluble solitary ES Michaelis complex. Under these conditions the slope is K_I/K_M. As discussed in the text, other results are inconsistent with this interpretation, and alternative mechanism is suggested. (B). Dependence of $X_I(50)$ of MJ33 (squares) and RM2 (circles) on the concentration of DC_8PM present as micelles. $X_I(50)$ is calculated by subtracting cmc (= 0.35 mM) from the bulk lipid concentration.

The bulk saturating concentrations of substrates (Figure 2) are above their cmc's. Since a pre-formed interface is present in micelles and vesicles, dependence of the observed rate on the inhibitor concentration may be meaningfully expressed in the interfacial concentration units such as X_I-(50), the mole fraction for 50% inhibition. This is based on the assumption that the catalysis occurs at the interface and that all the inhibitor is partitioned in the interface. The partition coefficient of MJ33 and RM2 in favor of the micellar interface is very high (Jain et al., 1993b). Thus $I_c(50)$ values obtained above cmc can be expressed as X_I-(50) values by taking into consideration only the substrate concentration present as micelles, that is, cmc subtracted from the bulk concentration, or by taking into account only the substrate concentration present in the outer monolayer of vesicles. As shown in Figure 4C the $X_I(50)$ values are constant as a function of the bulk substrate concentration above cmc. This is an expected result for interfacial catalysis because the interfacial substrate concentration that the enzyme "sees" for the formation of the Michaelis complex does not change with the bulk concentration of the substrate (Jain et al., 1986a, 1995; Berg et al., 1991).

The interfacial K_M* is related to $X_I(50)$ (Berg et al., 1991)

$$1 + \frac{1}{K_M^*} = \left(1 + \frac{1}{K_I^*}\right)\left(\frac{X_I(50)}{1 - X_I(50)}\right) \quad (3)$$

K_M* values obtained from the K_I* values, determined by the protection method (Jain et al., 1991b), are summarized in Tables 1 and 2. These values are in agreement with the K_M* values obtained from K_{Ca}*(S). From Table 2 it is clear that K_M* values display only a modest dependence on the structure of the head group. Based on these results, k_{cat} was calculated from V_M^{app} and K_M* value according to the equation:

$$k_{cat} = V_M^{app}(1 + K_M^*) \quad (4)$$

Results summarized in Table 2 show that the lower V_M^{app} for the hydrolysis of arsonolipids is primarily due to low k_{cat}. As also summarized in Table 2, the interfacial equilibrium dissociation constants for the products of hydrolysis (K_P*) of *R*-arsonolipid and phospholipid and for the nonhydrolyzable substrate analog, the *S*-enantiomer (K_S*), are comparable. These values are also comparable to those with long-chain phospholipids. Collectively these results show that the primary effect of the change in the structure of the head group is on the chemical step of the catalytic cycle. The change in K_M*, at least in part, is due to the change in the value of k_2 (which is k_{cat}), because

$$K_M^* = \frac{k_2 + k_{-1}}{k_1} \quad (5)$$

For DC_8PM $k_{-1} \ll k_1$, based on $K_S = k_{-1}/k_1 = 0.004$ (Table 2).

Aggregation Tendency of DC_8PM and PLA_2. The cmc values obtained by surface tension measurement are in agreement with those obtained by inflection of $I_c(50)$ versus DC_8PM concentration (Figure 4A). The surface tension method was employed to monitor a change in the monomer substrate concentration, which provides information about the effects of enzyme and inhibitor on the aggregation tendency of the substrate. Nonhydrolyzable DC_8PM-ether (cmc of 0.03 mM) was employed for the measurements in the presence of the enzyme. In the presence of PLA_2 the inflection shifts to 0.12 mM (results not shown). This effect of the enzyme can be rationalized as a competition for the amphiphile between the air/water surface versus the enzyme in the bulk aqueous phase. Thus the air/water surface effectively saturates at higher DC_8PM-ether concentrations as the enzyme binds the monomeric amphiphile. This shifts the natural equilibrium between surface monomers and micelles. Since the apparent cmc increases from 0.03 to 0.12 mM in the presence of 0.00465 mM PLA_2, these results show that the mole ratio of lipid to enzyme in the aggregate is about 20, as also shown by the fluorescence method, described below. These results support the hypothesis that premicellar aggregates of PLA_2 are formed with monomeric amphiphiles and show that the enzyme alone or in combination with the amphiphiles does not partition in the air/water interface.

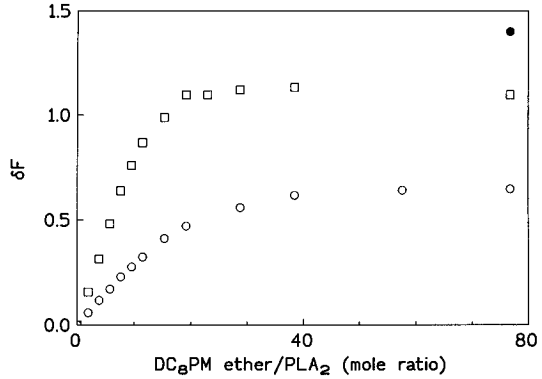

FIGURE 5: Change in fluorescence emission at 333 nm for pig pancreatic PLA_2 (excited at 280 nm) as a function of DC_8PM-ether (expressed as lipid/enzyme mole ratio). Pig PLA_2 (1.77 μM) was preequilibrated in a 1.4 mL cuvette containing 5 mM NaCl and 10 mM Tris buffer with background levels of Ca(II) (squares) or with 2.4 mM EGTA (circles), at pH 8.0 and 25 °C. $CaCl_2$ (2.86 mM) was added at the end of the titration containing EGTA (filled circle). Fluorescence measurements were taken after each successive addition of DC_8PM-ether.

High Affinity Binding of PLA_2 to Substrate below Its Cmc. Binding of PLA_2 to the interface is accompanied by an increase in the fluorescence emission from Trp-3 (Jain et al., 1982, 1986b; Jain & Vaz, 1987; Jain & Berg 1989). As shown in Figure 5, the fluorescence intensity increases linearly with the bulk DC_8PM-ether concentration and reaches maximum at roughly 20 amphiphile molecules per enzyme. This corresponds to a bulk concentration of DC_8-PM-ether of roughly 0.023 mM, which is slightly below cmc; however, it may be noted that the lipid/enzyme ratio of 20 is observed even if the enzyme concentration is increased by a factor of 10. If microaggregates were not formed, there should be no increase in the fluorescence until cmc of DC_8-PM-ether (0.03 mM) is reached. Results show not only an increase but also a saturation below cmc with no further increase in the fluorescence above cmc.

Spectroscopic Signatures of PLA_2 in Premicellar Aggregates. Binding of an active site-directed ligand to PLA_2 at the interface is accompanied by a characteristic change in the UV absorbance; however, such changes are not seen with a monodisperse EL complex. As shown in Figure 6, the change in the UV absorbance on the binding of PLA_2 to DC_6PM-ether (or DC_8PM-ether) showed a change charac-

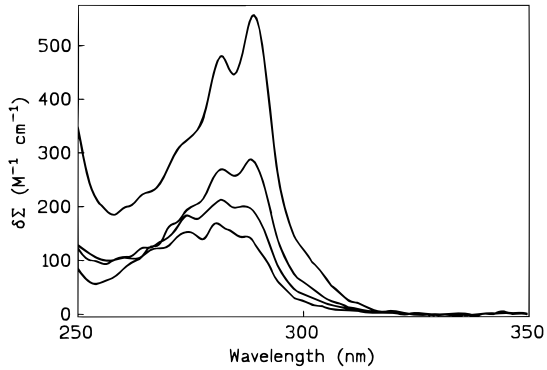

FIGURE 6: Change in the absorbance spectrum on the addition of (from top) 1070, 535, 214, and 107 nmol of DC_6PM-ether added to 21 nmol of pig PLA_2 in 0.6 mL of 10 mM Tris [with background levels of Ca(II)] at pH 8.0 and 24 °C. Such spectral changes are observed only upon the formation of E*L species [see Jain and Maliwal, (1993)].

teristic for the occupancy of the active site as in E*L. Not only the fine structure of the spectral change is different for these two lipids, but the shape and the magnitude of the absorbance change is also different than that observed with the E* to E*L change on a neutral diluent (Dupureur et al., 1992). Regardless of whether such changes could arise from a difference in the microenvironment of the tryptophan and tyrosine residues involved in these interactions, it is clear that changes in the UV spectrum are associated with the binding of an active site directed ligand to the enzyme at the interface because such spectral changes are not seen on the binding of an active site-directed ligand to the enzyme in the aqueous phase (Jain et al., 1993b).

DISCUSSION

The study described in this paper was designed to understand the role of the *sn*-3 phosphate of the substrate in the events of the interfacial catalytic cycle. Protocols to deconvolute relevant parameters for the hydrolysis of short chain anionic lipids are also developed. The surprising results are that PLA2 forms premicellar aggregates, that the rate of hydrolysis does not show an anomalous effect at the cmc of the bulk substrate, and that the chemical step of the catalytic cycle is significantly influenced by the nature of the polar substituent. The detailed significance of these observations in the context of interfacial catalysis is developed below.

Hydrolysis Occurs in Aggregates. Binding of PLA_2 to the interface is a critical step for interfacial catalysis. Results reported here show that while the bulk of the short chain substrate molecules are dispersed as solitary monomers below their critical micelle concentration, the microenvironment of the enzyme where catalysis occurs is similar to that of an aggregate. A plot of rate versus concentration of DC_8PM (Figure 2) and its phosphono- and arsonolipid analogs exhibits apparently classical hyperbolic dependence with no apparent anomalous effect at cmc. While these results are consistent with the effect of pancreatic PLA_2 on anionic sulfolipids (Van Oort et al., 1985), this apparently standard substrate concentration dependence has a quite different microscopic significance due to the formation of premicellar aggregates.

The hyperbolic dependence of the observed rate on the concentration of anionic substrates is quite different than that

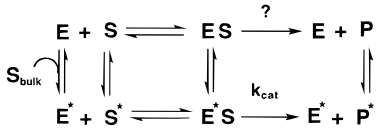

FIGURE 7: Minimum kinetic scheme for the hydrolysis of short chain phospholipids where the catalytic turnover may be mediated by the solitary monomer form (ES) or the interfacial form (E*S) of the Michaelis−Menten complex. In analogy with the classical Michaelis−Menten kinetics the catalytic turnover cycle with the ES form occurs in the aqueous phase. The E*S form mediates the catalytic turnover at the interface where not only the form of the enzyme but also the constraints of the binding of the substrate to form the E*S complex are controlled by the interface.

seen for the hydrolysis of short chain zwitterionic phosphatidylcholines by pancreatic PLA_2 where a dramatic increase in the rate is observed at the cmc (de Haas et al., 1971; Pieterson et al., 1974). Although the anomalous behavior at the cmc has been a holy grail of interfacial activation (Verheij et al., 1981), examination and evaluation of such results in terms of the constraints of interfacial catalysis on micelles remains a major unresolved issue in interfacial enzymology. A minimum kinetic model to facilitate discussion is shown in Figure 7. It consists of two parallel pathways for the hydrolysis of the substrate, and the molecular species involved in both of these pathways are assumed to be in equilibrium. One branch describes catalytic turnover via solitary monomeric Michaelis complex (ES) in the bulk aqueous phase and the other via the interfacial Michaelis complex (E*S) at the interface. Not only the state (conformational or allosteric) of the enzyme but also the effective substrate concentration for the formation of the Michaelis complexes during the catalytic turnover is different in the solitary and interfacial modes (Jain et al., 1993b). According to the scheme in Figure 7, hydrolysis of short chain phosphatidylcholines is interpreted with the assumption that below cmc the monomeric mode of hydrolysis predominates, whereas the interfacial mode on micelles predominates above the cmc (Pieterson et al., 1974; Verheij et al., 1981; Roberts, 1991). Serious doubt regarding this interpretation has been raised elsewhere (Rogers et al., 1992), and results reported in this paper show that indeed even when bulk of the DC_8PM is dispersed as solitary monomer the enzyme is present substantially, if not exclusively, in an aggregate formed with the substrate amphiphiles. Although we do not have any information about the structure and composition of these aggregates, from the bulk of the evidence it is clear that the overall process may be analogous to that of the formation of premicellar aggregates containing less than 100 amphiphiles per enzyme (Van Eyk et al., 1984; Van Oort et al., 1985). The kinetic results also suggest that the environment that the PLA_2 "sees" during the catalytic turnover on these micelles at saturating bulk substrate concentrations is comparable to what the enzyme "sees" on the interface during catalysis in the highly processive scooting mode (Jain et al., 1995).

The Chemical Step and the Transition State. V_M^{app} for the hydrolysis of DC_8PM is among the highest reported for PLA_2. Under these conditions the chemical step remains rate-limiting (Figure 2 and Table 1) as is the case at the bilayer interface (Jain et al., 1992). As a first approximation we have assumed that the substrate replenishment or removal of the product is rapid compared to the chemical step, and such physical processes do not contribute to the catalytic

turnover. If so, V_M^{app} corresponds to the interfacial turnover rate at maximum mole fraction (= 1) of the substrate expressed as υ_o. The fact that the chemical step remains rate-limiting at saturating bulk substrate concentrations is consistent with the assumption that the effective rate of replenishment of the substrate in the premicellar complex is considerably more rapid than the rate of hydrolysis. For example, in micelles of DC_8PM with cmc of about 10^{-4} M, the effective exchange rate is expected to exceed 10^5 s^{-1}. This is based on the general observation that in micelles the on-rate for the binding of an amphiphile is diffusion-limited and that the effective exchange rate is limited by the off-rate for the removal of the amphiphile from the interface as implicit in the value of cmc. This extrapolation from the behavior of micelles is valid only if the exchange properties of the amphipile in the enzyme-containing aggregates are the same as in the micelles without enzyme. While this assumption is probably valid at saturating bulk substrate concentrations, the bulk substrate concentration dependence of the rate (Figure 2) suggests that at low bulk substrate substrate concentrations this assumption is not valid and we are trying to evaluate its significance.

Collectively, the results at hand show that the observed rate for the hydrolysis of anionic amphiphiles is predominantly, if not exclusively, due to catalytic turnover through the interfacial E*S form of PLA_2, and that the turnover through the monomeric ES form, if it occurs at all, is relatively insignificant and cannot be deconvoluted. It is also obvious that for a quantitative interpretation of the significance of K_M^{app} and V_M^{app} it will be necessary to have an estimate of the structure, size, and exchange dynamics of the components in the complex where the catalytic turnover occurs.

Implications on the Reaction Mechanism and the Nature of the Transition State. The rate constant for the chemical step, k_{cat} (= k_2 on the basis of oxy/thio ratio), changes significantly with the structure of the head group. Also, there is a small difference in K_S* values which would suggest that the partitioning of E*S changes with the nature of the substrate. This conclusion is not entirely consistent with the current consensus mechanism for secreted PLA_2 (Verheij et al., 1980; Scott et al., 1990), which postulates that the *sn*-3 phosphate is required for the formation of the Michaelis complex. According to this mechanism Ca(II) polarizes the carbonyl group as a prelude to the formation of the transition state intermediate, formed by an attack by a water molecule (or hydroxide) activated by His-48. The fact that the rate of hydrolysis of the thio- substrate is considerably lower than that of the oxy- substrate (Jain et al., 1992) is also inconsistent with the consensus mechanism because a nucleophilic attack on the thioester group is favored. An attractive alternative or refinement for the current consensus mechanism is suggested by the results in this paper and the modeling studies described elsewhere (Seshadri et al., 1994). It is briefly outlined below while details are being worked out.

The question of the rate-limiting step in the catalytic mechanism of PLA2 has not been addressed before because the primary rate and equilibrium parameters could not be determined. This has been accomplished by the use of highly processive scooting kinetics (Jain et al., 1995), and an attempt to integrate this information is shown in Figure 8. Here, calcium is responsible for the formation and

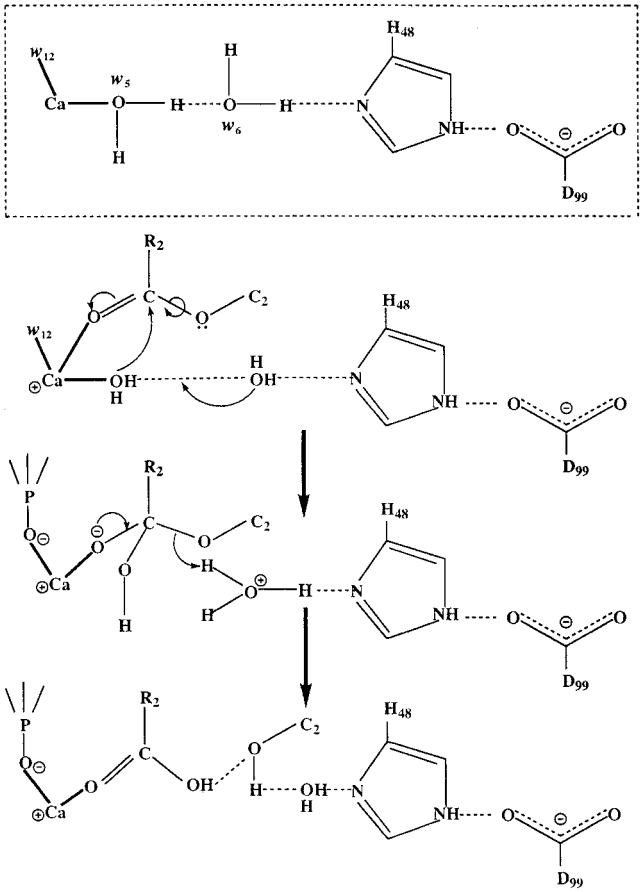

FIGURE 8: Top panel (in the box) shows the relationship of the catalytic residue (His-48), the calcium cofactor, and the three water molecules in PLA_2 as shown by crystallographic results (Dijkstra et al., 1983; Scott et al., 1990). Next three panels show possible sequence of events during the chemical step of the catalytic cycle by PLA_2. Initial binding of the substrate carbonyl occurs such that (first step) w_5 in the coordination shell is the nucleophile. Decomposition of the tetrahedral intermediate (second step) is initiated as the oxygen of the *sn*-3 phosphate displaces w_{12}. This is postulated to be the rate-limiting step.

localization of the nucleophile that attacks the *sn*-2 carbonyl group to form the tetrahedral transition intermediate. Details of the model are being worked out; however, key elements may be noted. It is postulated that neither the formation of the nucleophile nor its attack on the *sn*-2 carbonyl group is the rate-limiting step, but it is in the decomposition of the tetrahedral intermediate. Since polarized w_5 in the expanded coordination shell is hydrogen-bonded to δN of H48 via w_6 (Figure 8), it is likely that as w_5 is deprotonated by the calcium ion (with a possible contribution from D49), the resulting nucleophilic hydroxide (still in the coordination shell) attacks the carbonyl to form the tetrahedral intermediate. Then, in the rate-limiting step, *pro-S* oxygen from the *sn*-3 phosphate replaces apical w_{12} to enhance the decomposition of the transition state intermediate into products. The catalytic water invoked in this mechanism will not be seen in the structure of cocrystals because the extra oxygen in the tetrahedral phosphate (Scott et al., 1990) or the hydrogen-bonding of the amide nitrogen with H-48 (Thunnissen et al., 1990) would disrupt the hydrogen-bonding network stabilizing w_5 in the coordination shell around the Ca.

To recapitulate, results reported here show that hydrolysis of anionic phospholipids occurs in aggregate form of the

substrate even when bulk of the substrate is dispersed as solitary monomer. Since the k_{cat} depends on the nature of the head group (phosphate, phosphonate, arsonate), it is suggested that its interaction with Ca(II) is critical in the chemical step of the catalytic cycle, possibly during the decomposition of the tetrahedral transition intermediate.

ACKNOWLEDGMENT

We are grateful to Dr Otto Berg for his critically useful comments and suggestions during the course of this work.

REFERENCES

Berg, O. G., Yu, B. Z., Rogers, J., & Jain, M. K. (1991) *Biochemistry 30*, 7283−7297.
Cajal, Y., Ghanta, J., Easwaran, K., Surolia, A., & Jain, M. K. (1996) *Biochemistry 35*, 5684−5695.
de Haas, G. H., Bonsen, P. P. M., Pieterson, W. A., & Van Deenen, L. L. M. (1971) *Biochim. Biophys. Acta 239*, 252−266.
Dijkstra, B. W., Renetseder, R., Kalk, K. H., Hol, W. G. J., & Drenth, J. (1983) *J. Mol. Biol. 147*, 97−123.
Dupureur, C. M., Yu, B. Z., Jain, M. K., Noel, J. P., Deng, T., Li, Y., Byeon, I. L., & Tsai, M. D. (1992) *Biochemistry 31*, 6402−6413.
Eibl, H. (1980) *Chem. Phys. Lipids 26*, 405−428.
Gelb, M. H., Jain, M. K., Hanel, A. M., & Berg, O. G. (1995) *Annu. Rev. Biochem. 64*, 653−688.
Jain, M. K., & Vaz, W. L. C. (1987) *Biochim. Biophys. Acta 905*, 1−8.
Jain, M. K., & Berg, O. G. (1989) *Biochim. Biophys. Acta 1002*, 127−156.
Jain, M. K., & Rogers, J. (1989) *Biochim. Biophys. Acta 1003*, 91−97.
Jain, M. K., & Maliwal, B. P. (1993) *Biochemistry 32*, 11838−11846.
Jain, M. K., Egmond, M. R., Verheij, H. M., Apitz-Castro, R. J., Dijkman, R., & de Haas, G. H. (1982) *Biochim. Biophys. Acta 688*, 341−348.
Jain, M. K., Rogers, J., Jahagirdar, D. V., Marecek, J. F., & Ramirez F. (1986a) *Biochim. Biophys. Acta 860*, 435−447.
Jain, M. K., Rogers, J., Marecek, J. F., Ramirez, F., & Eibl, H. (1986b) *Biochim. Biophys. Acta 860*, 462−474.
Jain, M. K., Rogers, J., & de Haas, G. H. (1987) *Biochim. Biophys. Acta 940*, 51−62.
Jain, M. K., Yu, B. Z., Rogers, J. Ranadive, G. N., & Berg, O. G. (1991a) *Biochemistry 30*, 7306−7317.
Jain, M. K., Tao, W., Rogers, J., Arenson, C., Eibl, H., & Yu, B. Z. (1991b) *Biochemistry 30*, 10256−10268.
Jain, M. K., Rogers, J., Berg, O., & Gelb, M. H. (1991c) *Biochemistry 30*, 7340−7348.
Jain, M. K., Yu, B. Z., Rogers, J., Gelb, M., Tsai, M. D., Hendrickson, E. K., & Hendrickson, H. S. (1992) *Biochemistry 31*, 7841−7847.
Jain, M. K., Rogers, J., Hendrickson, H. S., & Berg, O. G. (1993a) *Biochemistry 32*, 8360−8367.
Jain, M. K., Yu, B. Z., & Berg, O. G. (1993b) *Biochemistry 32*, 11319−11329.
Jain, M. K., Gelb, M. H., Rogers, J., & Berg, O. G. (1995) *Methods Enzymol. 249*, 567−614.
Kuipers, O. P., Dekker, N., Verheij, H. M., & de Haas, G. H. (1990) *Biochemistry 29*, 6094−6102.
Lacoste, A.-M., Dumora, C., Ali, B. R. S., Neuzil, E., & Dixon, H. B. F. (1992) *J. Gen. Microbiol. 138*, 1283−1287.
Lewis, K. A., Bian, J., Sweeney, A., & Roberts, M. F. (1990) *Biochemistry 29*, 9962−9970.
Long, J. W., & Ray, W. J., Jr. (1973) *Biochemistry 12*, 3932−3938.
Pieterson, W. A., Vidal, J. C., Volwerk, J. J., & de Haas, G. H. (1974) *Biochemistry 13*, 1455−1460.
Roberts, M. F. (1991) *Methods Enzymol. 197*, 95−112.
Rogers, J., Yu, B. Z., & Jain, M. K. (1992) *Biochemistry 31*, 6056−6062.
Rosenthal, A. F., Vargas, L. A., Isaacson, Y. A., & Bittman, R. (1975) *Tetrahedron Lett.*, 977−980.
Schwartz, P. W., Tropp, B. E., & Engel, R. (1988) *Chem. Phys. Lipids 49*, 1−7.
Scott, D. L., White, S. P., Otwinowski, Z., Yuan, W., Gelb, M. H., & Sigler, P. B. (1990) *Science 250*, 1541−1546.
Serves, S. V., Tsivgoulis, G. M., Sotiropoulos, D. N., Ioannou, P. V., & Jain, M. K. (1992) *Phosphorus, Sulfur, Silicon 71*, 99−105.
Serves, S. V., Sotiropoulos, D. N., Ioannou, P. V., & Jain, M. K. (1993) *Phosphorus, Sulfur, Silicon 81*, 181−190.
Serves, S. V., Sotiropoulos, D. N., & Ioannou, P. V. (1995) *Phosphorus, Sulfur Silicon 106*, 75−77.
Seshadri, K., Vishveshwara, S., & Jain, M. K. (1994) *Proc. Indian Acad. Sci. 106*, 1177−1189.
Soltys, C. E., & Roberts, M. F. (1994) *Biochemistry 33*, 11608−11617.
Tausk, R. J. M., Karmigglt, J., Oudshoorn, C., & Overbeek, J. T. G. (1974) *Biophys. Chem. 1*, 175−183.
Thunnissen, M. M. G. M., Ab, E., Kalk, K. H., Drenth, J., Dijkstra, B. W., Kuipers, O. P., Dijkman, R., de Haas, G. H., & Verheij, H. M. (1990) *Nature 347*, 689−691.
Tsien, R., & Pozzan, T. (1989) *Methods Enzymol. 172*, 230−262.
Tsivgoulis, G. M., Sotiropoulos, D. N., & Ioannou, P. V. (1991) *Phosphorus, Sulfur, Silicon 63*, 329−334.
Van Eyk, J. H., Verheij, H. M., & de Haas, G. H. (1984) *Eur. J. Biochem. 140*, 407−413.
Van Oort, M. G., Dijkman, R., Hille, J. D. R., & de Haas, G. H. (1985) *Biochemistry 24*, 7993−7999.
Verheij, H. M., Slotboom, A. J., & de Haas, G. H. (1981) *Rev. Physiol. Biochem. Pharmacol. 91*, 91−203.
Yu, B. Z., Berg, O. G., & Jain, M. K. (1993) *Biochemistry 32*, 6485−6492.

BI960526P